Electrical Properties of Hydrides and Deuterides of Zirconium*

P. W. BICKEL†
Atomics International, Division of North American Rockwell, Canoga Park, California 91304
AND
T. G. BERLINCOURT‡
Science Center, North American Rockwell, Thousand Oaks, California 91360

(Received 10 June 1970)

Electrical properties of hydrides and deuterides of zirconium have been investigated between 1.1 and 410°K. The metallic nature of these materials is evident in the fact that for compositions approaching ZrH_2, the hydride is a better conductor than is high-purity zirconium. Above ~150°K the electrical resistivity exhibits an interesting upturn, which arises from scattering from the optical-mode lattice vibrations. Excellent fits to the ideal-resistivity data are obtained with a simple additive combination of Grüneisen and Howarth-Sondheimer functions for the respective acoustical- and optical-mode scattering contributions. The corresponding acoustical- and optical-mode characteristic temperatures are in good accord with expectations based on earlier inelastic neutron scattering data. Moreover, the optical-mode characteristic temperature exhibits the expected hydride-deuteride isotope shift of $\sqrt{2}$. The observed Hall coefficients are large in magnitude (much greater than for pure Zr), and indicate majority hole conduction for the fcc δ phase and majority electron conduction for the face-centered tetragonal ϵ phase. The thermoelectric power also changes from positive to negative with increasing hydrogen concentration in the range $ZrH_{1.5}$–ZrH_2.

I. INTRODUCTION

Zirconium hydride is widely employed as a neutron moderator in nuclear reactors, and accordingly its phase diagram,[1] thermal properties,[2,3] and neutron scattering characteristics[4–9] have been extensively investigated. The data presented below were obtained some ten years ago as part of a program to characterize this interesting material electrically as well. Because of the untimely death of P. W. Bickel this program was never fully completed, and publication of the results was limited to one brief note in the open literature[10] and a report to the United States Atomic Energy Commission.[11] Although other works on the electrical properties of zirconium hydride have appeared in the literature[12,13] in the intervening years and have confirmed the metallic nature of zirconium hydride, the results presented below remain by and large unduplicated.

Of particular interest is the reflection in the electrical resistivity of the unusual phonon dispersion which exists in zirconium hydride. Neutron scattering experiments first showed that the zirconium and hydrogen atoms occupy separate sublattices with the hydrogen atoms occupying tetrahedral lattice sites in fcc and face-centered tetragonal (fct) zirconium hydride (approximately $ZrH_{1.5}$–ZrH_2) and further that these hydrogen atoms behave to first approximation much like independent simple harmonic or "Einstein" oscillators. The level spacing of these Einstein or optical modes is ~0.137 eV, which is well above the acoustical-mode high-frequency cutoff of ~0.02 eV. In Ref. 10 the present authors reported observation of a prominent contribution to the electrical resistivity above ~150°K which could be attributed to scattering by these optical-mode phonons. Shortly thereafter contributions of the optical modes to the specific heat were observed by Flotow and Osborne[2] and by Tomasch[3] in both the hydride and deuteride, and the appropriate isotope shift of $\sqrt{2}$ was confirmed. The electrical resistivity data on zirconium deuteride reported below add further confirmation.

This work commenced with investigation of the electrical resistance and Hall coefficient as functions of temperature and composition for hydrogen-to-metal ratios H/M (deuterium-to-metal ratios D/M) greater than 1.5. Later, partly because of uncertainty regarding the influence of microcracks on these properties, the scope of this study was enlarged to include measurement of the thermoelectric power, a property less sensitive to the presence of such defects.

II. EXPERIMENTAL METHODS

A. Sample Preparation and Analysis

The amount of hydrogen that will combine with a specimen of zirconium is a function of the purity of the zirconium and hydrogen, the temperature, the hydrogen pressure, and the surface conditions.[14] The samples used in this study were prepared by a massive hydriding technique.[15] Clean specimens of reactor-grade zirconium were placed within a vacuum furnace and brought to hydriding temperature, typically 1450–1650°F. Purified hydrogen was then admitted in sufficient amount to achieve the desired H/M. Hydriding time for a typical specimen was of the order of 40 h, including cooling time.

An accurate knowledge of hydride composition is necessary if reliable interpretations are to be made from the electrical properties of the samples. In this study, the composition of each sample was determined from weight gain and also from vacuum fusion measurements. If any serious discrepancy existed, the sample was reanalyzed by the vacuum fusion method, which should have a reliability of ±1%. In all cases, the vacuum fusion analysis is the one reported.

TABLE I. Electrical resistivities, Hall coefficients, and crystal structures of zirconium hydride, zirconium deuteride, and zirconium.

Sample	T °K	$10^6\rho$ Ω cm	10^5R_H cm³/C	Structure by x rays
$ZrH_{1.54}$	1.1	44.5		fcc
	4.2	44.5	+29.9	
	77	49.2	+37.3	
	300	69.1	+34.8	
$ZrH_{1.59}$	4.2	52.4		fcc+fct
	77	56.7		
	300	75.6	+39.0	
$ZrH_{1.62}$	4.2	52.8		fcc
	77	56.6		
	300	75.3	+39.0	
$ZrH_{1.63}$	4.2	47.4		fcc
	77	51.1	+11.2	
	300	73.2	+21.2	
$ZrH_{1.64}$	1.1	43.8		fcc+fct
	4.2	43.8	+39.8	
	77	47.3	+39.8	
	300	66.6	+42.0	
$ZrH_{1.74}$	4.2	33.8		fct
	77	38.7	−32.2	
	300	60.2	−17.7	
$ZrH_{1.81}$	1.1	28.9		fct
	4.2	28.9	−48.7	
	77	33.2	−50.4	
	300	54.7	−39.0	
$ZrH_{1.87}$	4.2	22.8		
	77	27.6	−52.0	
	300	49.5	−45.8	
$ZrH_{1.90}$	4.2	16.5		fct
	77	19.3	−66.0	
	300	38.4	−61.2	
$ZrH_{1.96}$	1.1	4.31		
	4.2	4.31		
	77	7.82	−65.9	
	300	24.7	−67.9	
$ZrD_{1.54}$	4.2	39.4		fcc
	77	43.3		
	294	65.7		
$ZrD_{1.61}$	4.2	38.8		fcc
	77	42.3		
	294	62.6		
$ZrD_{1.74}$	4.2	42.6		fct
	77	46.0		
	295	67.5		
$ZrD_{1.76}$	4.2	43.6		fct
	77	47.5		
	295	67.5		
$ZrD_{1.79}$	4.2	24.8		fct
	77	28.8		
	294	51.2		
$ZrD_{1.84}$	4.2	22.9		
	77	26.7		
	294	47.5		
Zr (high purity)	4.2	0.213		hcp
	77	6.08		
	300	42.6		
Zr (reactor grade)	4.2	5.97		hcp
	77	12.8		
	300	50.8		

The as-hydrided specimens, either in the shape of small rectangular plates or cylindrical rods, were first cut to approximate size with a diamond cutoff wheel. Next, the sample was shaped to the desired dimensions by means of a polishing block and metallurgical paper. When finished, the samples were $\frac{7}{8}$ in. long by $\frac{1}{8}$ in. wide by 20–40 mil thick. These dimensions were established by the electrical and cryogenic equipment available for performance of the measurements. Since zirconium hydride is very brittle, especially for large H/M, it was necessary to handle the samples with great care throughout the preparation and data-gathering phases. In addition, it was found that unless the samples were etched, proper electrical contact could not be established. A suitable etchant consists of 5 parts HF, 45 parts HNO_3, and 50 parts H_2O by volume.

All samples studied were polycrystalline and contained appreciable numbers of microcracks as revealed by microscopic examination at magnifications of the order of 250×. Figure 1 is a photomicrograph of $ZrH_{1.81}$, a typical sample. The influence of these defects on the properties studied will be discussed later. The "banding" shown in this photograph is typical of high-hydrogen-content zirconium hydride. The effect of oxygen impurity variations on the electrical properties of the samples was not investigated.

B. Electrical Resistivity and Hall-Effect Measurement Techniques

Standard potentiometric techniques were used for the resistivity measurements, and the three-probe geometry[16] was employed for the Hall-effect measurements. The Hall voltage V_H was taken as one-half the difference in voltage measured by a μV potentiometer for forward and reverse magnetic field directions. Field reversal was actually accomplished by a 180° rotation of the sample about its long axis. In terms of the measured quantities, the Hall coefficient is given by $R_H = V_H t/IH$, where t is the sample thickness, I is the measuring current, and H is the magnetic field strength.

The voltage drops between resistivity probes varied from a few hundred to a thousand μV for measuring currents between 0.2 and 0.4 A. Hall voltages amounted to a few tenths of a μV and were reproducible to about 0.005 μV or better.

Electrical contacts to the edges of the sample were accomplished by means of spring clips. Even though the sample holder was constructed in such a way as to minimize constraint during thermal expansion and contraction of the samples, fracture of the brittle samples sometimes occurred. This difficulty is not easily overcome through the use of thicker samples, because the Hall voltage (which is small at best) is inversely proportional to the sample thickness.

The cryogenic and magnetic apparatus and procedures used in this investigation have been described elsewhere.[17,18]

C. Thermoelectric Power Measurement Techniques

The thermoelectric power measurements do not suffer from complications arising from the brittle nature of zirconium hydride, inasmuch as thin samples are not required, and microcracks are of less influence. The experimental apparatus is illustrated schematically in Fig. 2. With this arrangement, which was intended only for rapid exploratory measurements, it was possible to make measurements between 0 and 150°C. It was not convenient to vary each junction temperature separately, but this proved to be of little consequence because the thermoelectric force ΔV was measured for a temperature difference $\Delta T = T_1 - T_2$, and plots of $\Delta V/\Delta T$ versus average temperature $\frac{1}{2}(T_1+T_2)$ were linear in all cases. Under these circumstances, a plot of $\Delta V/\Delta T$ versus $\frac{1}{2}(T_1+T_2)$ is equivalent to a plot of thermoelectric power dV/dT versus T.

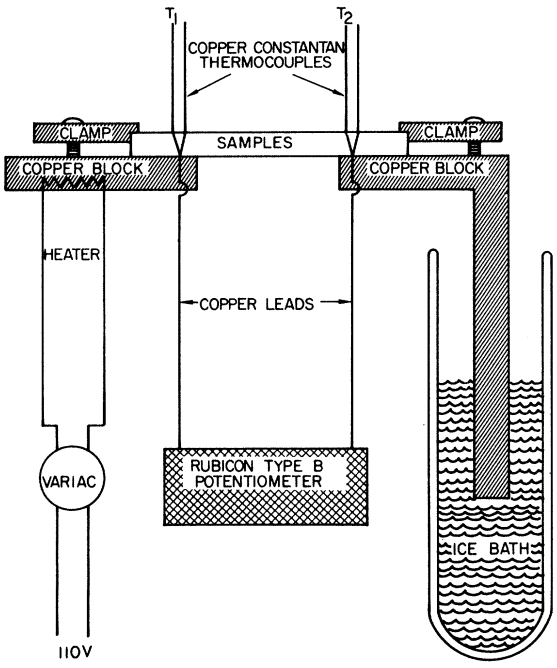

FIG. 2. Schematic diagram of thermoelectric power measurement apparatus.

All thermoelectric power measurements were made against copper. Between 0 and 100°C, the absolute thermoelectric power of copper in μV/°C is given[19,20] approximately by $1.5+0.0069T$ where T is in °C. This quantity was added to the measured thermoelectric power to yield the absolute thermoelectric power data for zirconium hydride reported in this paper.

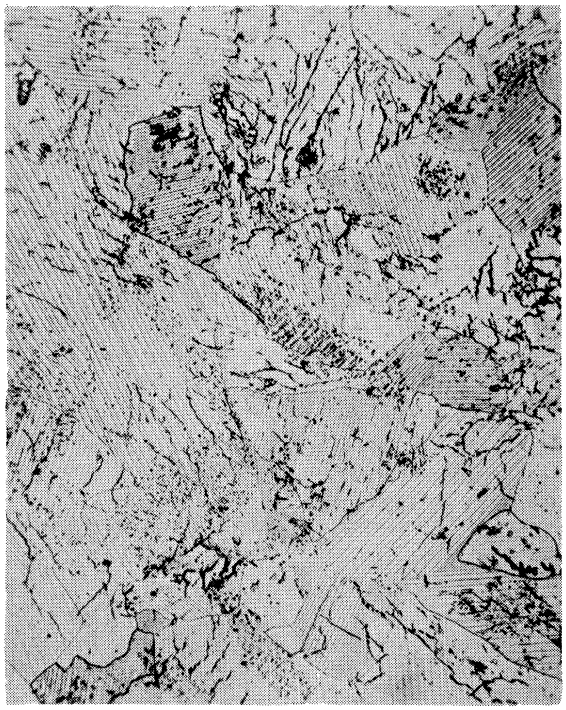

FIG. 1. Bright field photomicrograph of $ZrH_{1.81}$ for a magnification of 250×.

III. EXPERIMENTAL RESULTS AND DISCUSSION

A. Electrical Resistivity

Liquid-helium temperature, liquid-nitrogen temperature, and room-temperature values for the electrical resistivities of hydrides and deuterides of zirconium are presented in Table I together with information on crystal structures. (Data on high-purity and reactor-grade zirconium are included for comparison.) Reasonable agreement with other hydride determinations[12,13] is evident in the ranges of overlap. As previously noted, the specimens contained fair numbers of microcracks. Nevertheless, some confidence in the values listed in Table I is justified, because specimens cut from different portions of the same bar yielded resistivities in agreement within one percent or better, resistivity-versus-

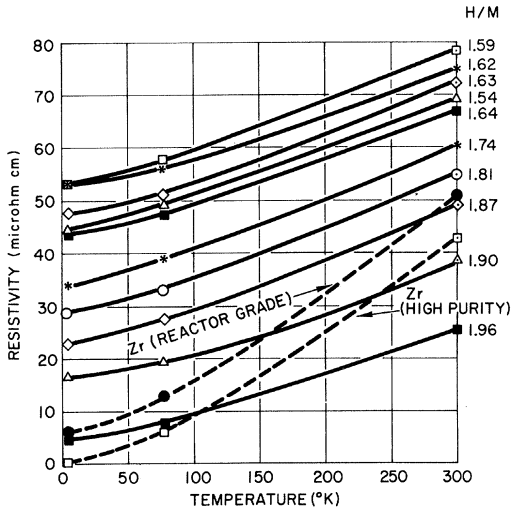

FIG. 3. Electrical resistivities of zirconium hydride and zirconium specimens at 4.2, 77, and 300°K.

concentration curves followed a regular course, and the observed resistivity at 4.2°K approached zero as stoichiometric ZrH_2 was approached.

Although electrical resistivity measurements were made down to 1.1°K for three zirconium hydride samples (Table I) no evidence of superconductivity was found, nor was a measurable magnetoresistance observable.

The zirconium hydride resistivity data from Table I are plotted against temperature in Fig. 3. The metallic nature of these materials is readily apparent. Indeed, as ZrH_2 is approached the hydride is a considerably better electrical conductor than is pure zirconium. Although the zirconium hydride curves appear to be approximately parallel to each other in Fig. 3, the more detailed data to be presented later indicate significant departures from this condition. Accordingly earlier conclusions[11] regarding the nature of the contribution of the hydrogen electron to the electronic structure which were based on parallelism of the resistivity curves now appear to be unwarranted.

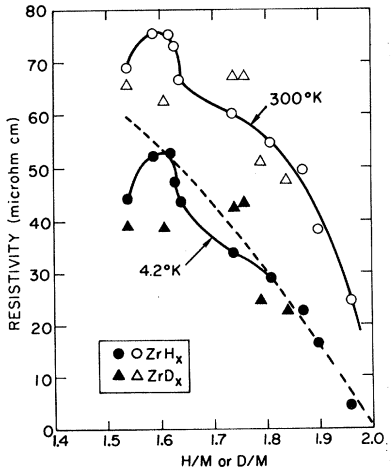

FIG. 4. Electrical resistivity versus composition for hydrides and deuterides of zirconium at 4.2 and 300°K. The dashed curve is proportional to $(H/2M)(1-H/2M)$.

In Fig. 4 the residual resistivity $\rho_r=\rho(4.2°K)$ and the room-temperature resistivity $\rho(300°K)$ are plotted against composition for the hydrides and deuterides. The differences evident between the ρ_r values for the hydrides and deuterides are puzzling in view of data[21] which suggest that the Zr-H and Zr-D phase diagrams are similar. Clearly more data are required to determine if these differences in ρ_r are genuine. Also puzzling is the bump in the hydride data below $H/M=1.65$. This could be associated with the change in crystal structure from fcc to fct with increasing hydrogen concentration and the existence of a concentration range where these two phases coexist. In such a two-phase region additional contributions to electron scattering would arise from phase boundaries and extra microcracks generated by thermal expansion mismatch.

TABLE II. Parameters used to fit Eq. (1) to experimental electrical resistivity data on polycrystalline zirconium hydride and zirconium deuteride.

	$ZrH_{1.54}$	$ZrH_{1.96}$	$ZrD_{1.84}$
a ($\mu\Omega$ cm)	19.17	11.96	16.16
b ($\mu\Omega$ cm)	18.35	15.06	31.4
Θ_ρ (°K)	225	200	210
Θ_E (°K)	1550	1550	1096
ρ_r ($\mu\Omega$ cm)	41.8	4.02	22.9

It is of interest to compare hydrogen vacancies in zirconium hydride with vacancies in pure metals as regards their effect on residual resistivity. By analogy with the case of simple solid solution alloy theory,[22] in the absence of impurities, changes in lattice parameter, and changes in number of charge carriers, the residual resistivity in zirconium hydride would be proportional to $x(1-x)$, where x is the fractional concentration of hydrogen vacancies (or in terms of H/M, $x=1-H/2M$). Such a dependence (fitted to the experimental point for $H/M=1.81$) has been plotted in Fig. 4 as the dashed line. This is a fair approximation to the 4.2°K data despite the obvious failure (see above) of the experimental system to fulfill the conditions imposed by the model. The slope of this dashed line at ZrH_2 yields a value of 3.3 $\mu\Omega$ cm/at.% vacancies relative to the hydrogen sublattice, or 2.2 $\mu\Omega$ cm/at. % vacancies relative to the entire lattice. Estimates of vacancy resistivities for pure noble metals range from 0.4 to 1.5 $\mu\Omega$ cm/at. % vacancies.[23] The values for zirconium hydride are surprisingly close to those for noble metals, in view of differences in electronic structure as indicated by the much lower ideal resistivities of the noble metals. It should be pointed out that the zirconium hydride

measurements enjoy some advantage over the determinations on pure metals, because in the former the vacancy concentration is known directly from the hydrogen concentration.

More detailed data on the temperature dependence of the ideal resistivity for $ZrH_{1.54}$, $ZrH_{1.96}$, and $ZrD_{1.84}$ are plotted in Figs. 5 and 6 where manifestations of both acoustical- and optical-mode scattering contributions are readily apparent. The plotted points represent the experimental data, while the solid curves represent parametrized theoretical fits based on the following simple model. If scattering by impurities (including hydrogen-deuterium vacancies) and by the acoustical and optical modes all make independent contributions, the electrical resistivity should be approximated by a function of the form

$$\rho=\rho_r+\rho_i=\rho_r+(aT/\Theta_\rho)g(\Theta_\rho/T)+bh(\Theta_E/T), \quad (1)$$

where ρ_r is the residual resistivity, ρ_i is the ideal resistivity, a and b are constants involving scattering cross sections and electronic factors, T is the temperature, $g(\Theta_\rho/T)$ is the well-known Grüneisen function[24] for acoustical-mode scattering, Θ_ρ is the acoustical resistive characteristic temperature,

$$h(\Theta_E/T)=[(T/\Theta_E)\sinh^2(\Theta_E/2T)]^{-1}$$

is the first-order approximation to the Howarth-Sondheimer function[25] for optical-mode scattering, and Θ_E is the optical-mode characteristic temperature. The function $h(\Theta_E/T)$ becomes appreciable only above about $0.1\Theta_E$.

The solid lines in Figs. 5 and 6 represent fits of Eq. (1) to the data using the parameters listed in Table II,

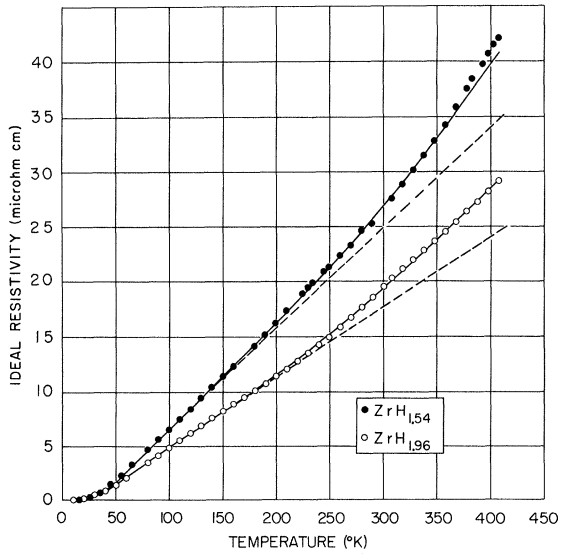

FIG. 5. Ideal resistivity versus temperature for $ZrH_{1.54}$ and $ZrH_{1.96}$. The solid lines represent fits of Eq. (1) to the experimental data, and the dashed lines represent the Grüneisen contributions alone.

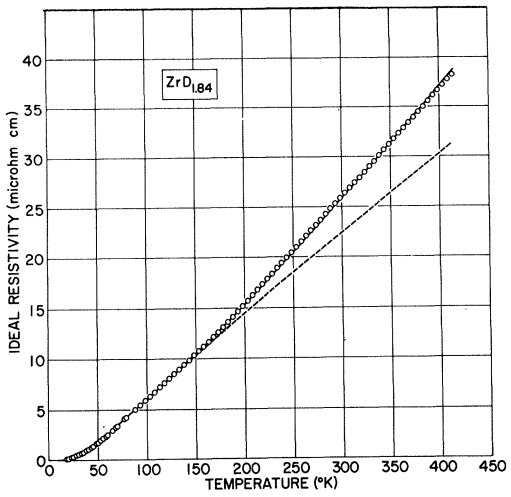

FIG. 6. Ideal resistivity versus temperature for $ZrD_{1.84}$. The solid line represents a fit of Eq. (1) to the experimental data, and the dashed line represents the Grüneisen contribution alone.

while the dashed line represents only the acoustical or Grüneisen contribution. The agreement is remarkably good in general, although a significant deviation exists at the highest temperatures for $ZrH_{1.54}$. Much larger deviations would not be unexpected in view of the possible lack of independence of the terms in Eq. (1) and evidence that the acoustical- and optical-mode dispersions which actually exist in zirconium hydride depart significantly from the "ideal" Debye and Einstein (δ-function) forms. A fair approximation to the neutron scattering data for the hydride consists of a Debye spectrum with a high-frequency cutoff at 0.02 eV (232°K) for the acoustical mode and a Gaussian distribution centered at 0.137 eV (1590°K) with a full width at half-maximum of 0.02 eV for the optical mode.[26] The Θ_ρ and Θ_E values used to fit Eq. (1) to the experimental resistivity data on zirconium hydride are in reasonable agreement, respectively, with these values for the Debye cutoff and the center of the optical-mode distribution. However, because four adjustable parameters (a, b, Θ_ρ, Θ_E) are used to fit Eq. (1) to the experimental data, variations of the order of $\pm 10\%$ in Θ_ρ and Θ_E do not degrade the agreement between theory and experiment appreciably. The difference between the hydride and deuteride is nonetheless readily distinguishable, and the lower Θ_E used to fit the deuteride resistivity data is in accord with both the expected hydride deuteride isotope shift of $\sqrt{2}$ and the results of neutron scattering experiments on the deuteride.[27] The present Θ_E determinations also show acceptable agreement with the specific-heat determinations of Flotow and Osborne[2] on the hydride and deuteride. However, for the acoustic-mode characteristic temperature the specific-heat measurements in the range below 11°K yielded the value 311°K, which is considerably greater than the values for Θ_ρ obtained in this work. In spite of this

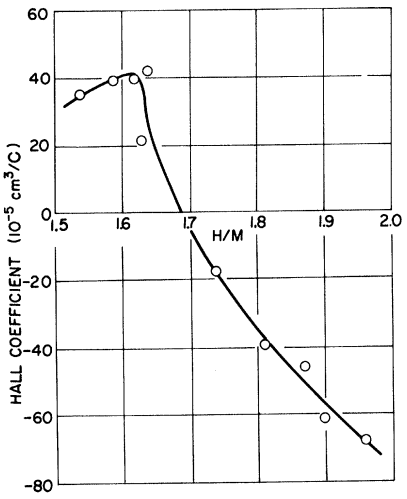

FIG. 7. Hall coefficient of zirconium hydride specimens versus composition at 300°K.

discrepancy the resistivity data presented here appear to confirm the existence of optical and acoustical modes which contribute in a quasi-independent fashion to the physical properties.

B. Hall Effect

In every case the Hall voltage was directly proportional to magnetic field strength throughout the range of measurement, 0–30 kG. The corresponding Hall coefficients are tabulated in Table I, and the 300°K data are presented graphically in Fig. 7. It is apparent that as the crystal structure changes from fcc to fct with increasing H/M the majority charge carriers change from holes to electrons. Interpreted in terms of a simple overlapping-electron-and-hole-band model this would imply that as hydrogen is added electrons are contributed to the Fermi sea. These electrons would reduce the number of holes in the hole band and increase the number of electrons in the electron band. However, a critical test of this hypothesis would require more detailed electron transport data than were obtained in this study.

C. Thermoelectric Power

As already indicated, the absolute thermoelectric power S was a linear function of temperature between 0 and 100°C for all zirconium hydride specimens studied and can therefore be represented by an equation of the form

$$S=A+BT, \qquad (2)$$

where A and B are constants characteristic of each specimen. The appropriate values for A and B for various H/M are listed in Table III, and values for S at 0 and 100°C are plotted against H/M in Fig. 8. The curves show positive thermoelectric powers for the lower H/M ratios and negative thermoelectric powers for the larger H/M ratios. This result is consistent with the simple overlapping-band picture discussed in Sec. III.B. However, it should be kept in mind that both the thermoelectric power and the Hall effect are often quite sensitive to small and very subtle changes in electronic structure and electron scattering,[17,28,29] and so the question of the manner in which hydrogen contributes electrons to the Fermi sea remains open.

TABLE III. Absolute thermoelectric power S of zirconium hydride specimens.

	$S=A+BT$		
Sample	10^6A V/°C	10^6B V/(°C)^2	Structure by x rays
$ZrH_{1.54}$	+19.4	−0.0241	fcc
$ZrH_{1.59}$	+20.5	+0.0189	fcc+fct
$ZrH_{1.62}$	+21.7	+0.0289	fcc
$ZrH_{1.63}$	+23.6	+0.0379	fcc
$ZrH_{1.64}$	+24.5	+0.0299	fcc+fct
$ZrH_{1.81}$	+4.2	−0.0091	fct
$ZrH_{1.90}$	−5.2	−0.0141	fct
$ZrH_{1.92}$	−5.4	−0.0271	
$ZrH_{1.96}$	−7.7	−0.0271	

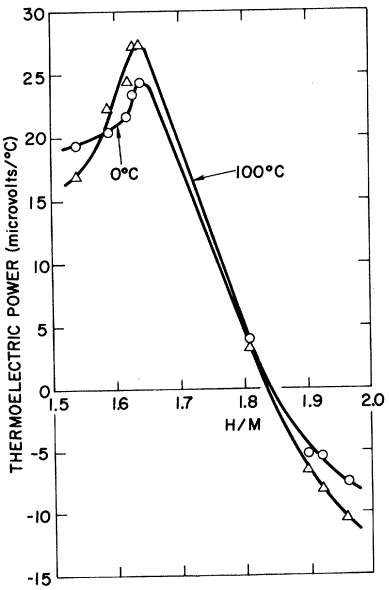

FIG. 8. Absolute thermoelectric power of zirconium hydride specimens versus compositio.. at 0 and 100°C.

IV. SUMMARY

The experimental data obtained in this investigation clearly demonstrate the metallic nature of the hydrides and deuterides of zirconium. The prominent role played by H or D vacancies in scattering electrons is readily apparent in the strong dependence of residual resistivity on H or D concentration. Acoustical- and optical-mode scattering contributions to the ideal resistivity were

separately identified, and the appropriate hydrogen-deuterium isotope shift was observed in the optical-mode characteristic temperature. The Hall effect and thermoelectric power data reveal majority hole conduction for the fcc hydride phase and majority electron conduction for the fct phase.

ACKNOWLEDGMENTS

We are indebted to G. W. Lehman and W. J. Tomasch for valuable discussions, to D. L. Henry for supplying specimens, and to D. H. Leslie for assistance with some of the measurements.

* Research supported in part by the U.S. Atomic Energy Commission.

† Deceased.

‡ Present address: Department of Physics, Colorado State University, Fort Collins, Colo. 80521.

[1] For references on the phase diagram of the Zr-H system see K. E. Moore and W. A. Young, J. Nucl. Mater. **27,** 316 (1968).

[2] H. E. Flotow and D. W. Osborne, J. Chem. Phys. **34,** 1418 (1961).

[3] W. J. Tomasch, Phys. Rev. **123,** 510 (1961).

[4] R. E. Rundle, C. G. Shull, and E. O. Woolan, Acta Cryst. **5,** 22 (1952).

[5] I. Pelah, C. M. Eisenhauer, D. J. Hughes, and H. Palevsky, Phys. Rev. **108,** 1091 (1957).

[6] A. Andresen, A. W. McReynolds, M. Nelkin, M. Rosenbluth, and W. Whittemore, Phys. Rev. **108,** 1092 (1957).

[7] W. L. Whittemore and A. W. McReynolds, Phys. Rev. **113,** 806 (1959).

[8] S. S. Sidhu, L. Heaton, and M. H. Mueller, J. Appl. Phys. **30,** 1323 (1959).

[9] For additional references on neutron scattering in zirconium hydride see S. S. Pan and F. J. Webb, J. Nucl. Sci. Eng. **23,** 194 (1965).

[10] P. W. Bickel and T. G. Berlincourt, Phys. Rev. **119,** 1603 (1960).

[11] P. W. Bickel, U.S. Atomic Energy Commission Report No. NAA-SR-4173, 1960 (unpublished).

[12] V. I. Savin, R. A. Andriyevskiy, Y. B. Boyko, and R. A. Lyutikov, Phys. Metals Metallog. (USSR) **24,** 54 (1967).

[13] R. A. Andrievskii, E. B. Boiko, and R. B. Ioffe, Izv. Akad. Nauk SSSR, Neorg. Mater. **3,** 1591 (1967).

[14] G. L. Miller, *Zirconium*, 2nd ed. (Academic, New York, 1957), pp. 267–272.

[15] J. B. Vetrano, U.S. Atomic Energy Commission Report No. BMI-1243, 1957 (unpublished).

[16] O. Lindberg, Proc. Inst. Radio Engrs. **40,** 1414 (1952).

[17] T. G. Berlincourt, Phys. Rev. **112,** 381 (1958).

[18] T. G. Berlincourt, Phys. Rev. **114,** 969 (1959).

[19] J. W. Christians, J. P. Jan, W. B. Pearson, and I. M. Templeton, Proc. Roy. Soc. (London) **A245,** 213 (1958).

[20] C. D. Hodgman, *Handbook of Chemistry and Physics*, 39th ed. (Chemical Rubber Publishing Co., Cleveland, 1957), p. 2234.

[21] K. P. Singh and J. Gordon Parr, Trans. Faraday Soc. **59,** 2256 (1963).

[22] N. F. Mott and H. Jones, *The Theory of the Properties of Metals and Alloys* (Dover, New York, 1936), pp. 296–300.

[23] G. J. Dienes and G. H. Vineyard, *Radiation Effects in Solids* (Interscience, New York, 1957), p. 66.

[24] N. F. Mott and H. Jones, *The Theory of the Properties of Metals and Alloys* (Dover, New York, 1936), Chap. 7, p. 240.

[25] D. J. Howarth and E. H. Sondheimer, Proc. Roy. Soc. (London) **A219,** 53 (1953).

[26] For a discussion of various models for the phonon dispersion in ZrH_2, see E. L. Slaggie, J. Phys. Chem. Solids **29,** 923 (1968).

[27] U. Schmidt, Atomkernenergie **12,** 385 (1967).

[28] B. R. Coles, Phys. Rev. **101,** 1254 (1956).

[29] A. H. Wilson, *The Theory of Metals*, 2nd ed. (Cambridge U. P., London, 1954), pp. 193–249.

PHYSICAL REVIEW B VOLUME 2, NUMBER 12 15 DECEMBER 1970

de Haas–van Alphen Effect in Platinum*

J. B. KETTERSON AND L. R. WINDMILLER

Argonne National Laboratory, Argonne, Illinois 60439

(Received 22 April 1970)

The de Haas–van Alphen effect has been used to study the extremal areas, cyclotron masses, and spin-splitting zeros on all three sheets of the Fermi surface of platinum. For the Γ-centered electron surface and *X*-centered hole pocket, newly developed inversion techniques have been employed to obtain the Fermi radius and Fermi velocity at all points on these surfaces. By performing the appropriate integrations over these surfaces, we have been able to determine the number of carriers and the density of states for these surfaces. Our observations on the open-hole surface, when combined with band-structure calculations, confirm the shape and connectivity of this surface. By combining effective-mass data with spin-splitting zero data, we have obtained information on the magnitude and anisotropy of the *g* factor on all surfaces. In general, we find the *g* factor to be different from 2.0 and quite anisotropic. The effective-mass measurements, when compared with band-structure calculations, indicate an enhancement of approximately 30%.

I. INTRODUCTION

The de Haas–van Alphen effect has proved to be a powerful tool for the determination of the Fermi surfaces of metals. Traditional measurements yield the cross-sectional areas of the Fermi surface in planes normal to the magnetic field. Recently however, this effect has been shown to be capable of yielding detailed measurements of the cyclotron mass, Dingle-Robinson temperature, and *g* factor of electrons on the Fermi surface. With such information available, studies of the de Haas–van Alphen (dHvA) effect in metals now appear useful not only for determining the shape of the Fermi surface, but also for determining the limitations of the one-electron model calculations and estimating the magnitude of the many-body interactions. Pt is a metal especially suitable for such a program since it is known from the heat capacity[1,2] and the magnetic sus-

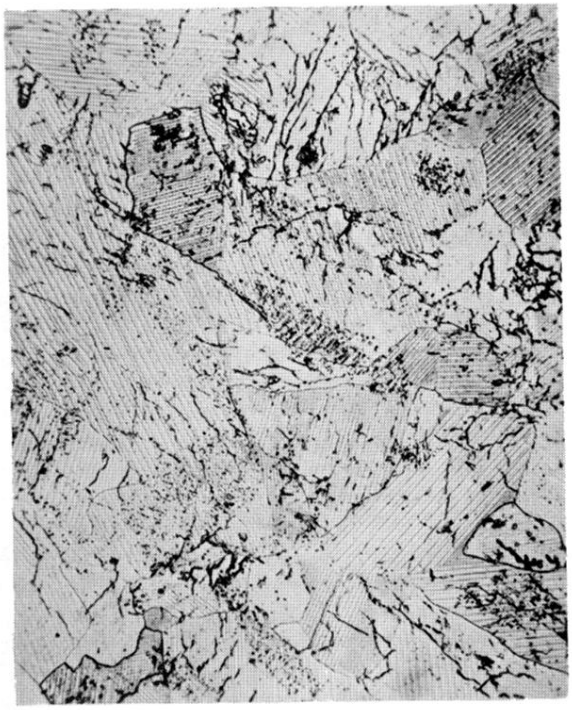

FIG. 1. Bright field photomicrograph of $ZrH_{1.81}$ for a magnification of 250×.